Polarization-Based Interference Mitigation for OFDM Signals in Channels with Polarization Mode Dispersion

Brett T. Walkenhorst and Thomas G. Pratt
Email: brett.walkenhorst@gtri.gatech.edu
Georgia Tech Research Institute
Atlanta, Georgia 30332–0855

***Abstract* — A dual-polarized antenna architecture is used in channels exhibiting polarization mode dispersion to investigate polarization-based interference suppression. In a wireless experiment, orthogonal frequency division multiplexing (OFDM) signals are transmitted from a slant-45° polarized antenna and received with a dual-polarized antenna. The vertical (V) and horizontal (H) received complex baseband samples are corrupted by synthesized broadband interference with arbitrary polarization. Channel estimates are formed for each subcarrier of the received OFDM signal and minimum mean-squared error (MMSE) weights are computed to maximize the signal to interference plus noise ratio (SINR) with a single interferer. We find that this sub-band processing approach improves the performance relative to full-band processing because of the polarization mode dispersion found in a typical wireless channel.**

***Index Terms* — Wireless communications, adaptive array, polarization, interference mitigation, OFDM.**

I. INTRODUCTION

Due to requirements for small form factors, the ETSI 3GPP group claims that polarized antennas are likely to be the primary method by which multiple antennas will be included on many mobile platforms [1]. This paper seeks to explore the use of polarization-based architectures in an interference limited environment by considering sub-banding to improve the performance of interference mitigation algorithms.

The use of polarization-based architectures for interference mitigation has distinct advantages over purely spatial diversity as noted by Compton [2]. For example, if two signals arrive at an array from very closely spaced incidence angles, a typical array will have difficulty differentiating between them. If these same signals have different polarizations, it may be possible to separate them or suppress one of them by using orthogonally polarized antenna elements in the array.

In polarization space, we are limited in the number of degrees of freedom available. Svantesson et al [10] demonstrate the theoretical possibility of six orthogonal polarizations using three electric dipoles and three magnetic dipoles; however, given the current state of technology, for most practical systems, we are limited to two orthogonal polarizations and this paper will consider such a dual-polarized architecture. Consequently, using purely polarization-based processing, we can typically cancel only a single interferer. When the interference environment becomes more complicated (as it often does), the designer will have to consider other dimensions of processing such as space, beam, successive interference cancellation, etc. The scope of this paper, however, addresses only polarization processing, so we limit ourselves to cancelling a single interference source.

It has been observed in measured data that a signal passed through a simple wireless channel experiences polarization mode dispersion (PMD) similar to that observed in a single mode optical fiber. Because of this PMD, the typical full-band processing [3-5] that is usually used for suppression is suboptimal for wideband signals. Sub-band processing is preferable since the dispersion over a small frequency band is negligible compared with the entire band. Therefore, the use of a frequency-domain polarization filter is proposed to exploit the frequency-dependent nature of the polarization state. Gasiewski et al consider sub-banding and polarization-based processing for interference mitigation, but do not appear to combine the two [6]. Fante briefly mentions the possibility of using a space-frequency-polarization filter by means of the fast Fourier transform, but does not report any results of such a scheme [7].

This paper explores the idea of polarization-frequency processing for interference suppression using orthogonal frequency division multiplexed (OFDM) data. The OFDM subcarrier channel estimates can be used to perform polarization-based processing on each subcarrier. The feasibility of the approach is demonstrated in experiments involving the collection of an OFDM signal using a slant-45° polarized antenna for transmission to provide approximately equal power at the vertical (V) and horizontal (H) ports of the dual-polarized receive antennas. The data format and collection system are described in Section II. A simple method of processing the OFDM subchannels is described in Section III with results and analysis outlined in Section IV. Section V presents the conclusions of the research.

II. COLLECTION SYSTEM AND DATA FORMAT

The OFDM signals utilized in the experiments have a bandwidth of 18 MHz with 256 subcarriers. 200 of the subcarriers carry data from a 64QAM constellation and 56 are zero-padded. A single OFDM symbol is defined in this way and repeated 40 times in a frame. The preamble consists of a synchronization word and the 802.16 short and long preamble for channel estimation. This OFDM signal is synthesized in MatLab and transmitted via an Agilent ESG-4438C signal generator at approximately a slant-45° polarization. Some of the basic OFDM parameters are listed in Table 1.

Prepared through collaborative participation in the Communications and Networks Consortium sponsored by the U. S. Army Research Laboratory under the Collaborative Technology Alliance Program, Cooperative Agreement DAAD19-01-2-0011. The U. S. Government is authorized to reproduce and distribute reprints for Government purposes notwithstanding any copyright notation thereon.

978-1-4244-2677-5/08/$25.00 ©2008 IEEE

Table 1. OFDM System Parameters

FFT block size	256
Cyclic prefix length	64
OFDM symbol size	320
Number of data-carrying subcarriers	200
Carrier frequency	2435 MHz
Signal bandwidth	14.0625 MHz
Sample rate	18 Msamples/s
Modulation	64-QAM
Frame preamble	Based on IEEE 802.16 standard

The receiver is composed of a dual-polarized antenna and a two-channel data acquisition board. The data is digitized, downconverted, decimated, and ported to a PC for offline processing. The OFDM format and collection system details are outlined more completely in [8]. The data was collected in a short range line-of-sight channel in the Software Radio Laboratory at Georgia Tech.

The received signal has a fairly high signal to noise ratio, possibly as high as 40dB, and can be demodulated using either of the two polarization states at the receiver. The plot in Figure 1 shows the soft decisions of a demodulated frame using the horizontally polarized component. The blue dots indicate received soft decisions and the green circles are the transmitted symbol positions.

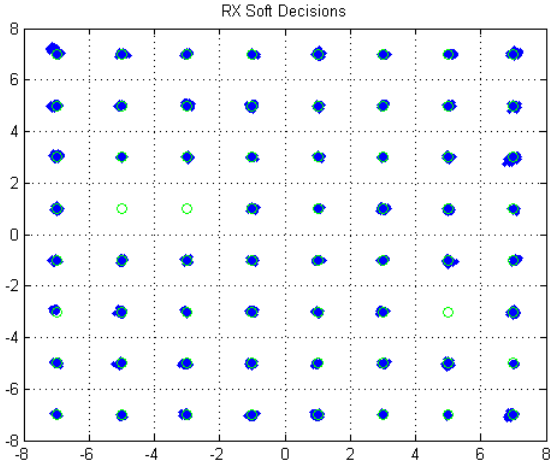

Figure 1. Soft decisions of a single OFDM frame with horizontal receive polarization.

Recall that the frame is composed of a single OFDM symbol repeated 40 times. In that one OFDM symbol, three of the 64QAM symbols are not used at all (they were randomly generated), so they appear nowhere in the demodulated signal.

Using the subcarrier channel estimates associated with each of the two receive polarization components, the polarization state of the OFDM symbol can be plotted as a function of subcarrier frequency on the Poincaré sphere. Figure 2 shows the resulting PMD observed in the received signal.

In Figure 2, the reference for vertical polarization is given by the green circle in the center of the plot. Horizontal polarization is on the opposite side of the sphere and is hidden from the shown perspective. The polarization states of the received signal subcarriers are indicated with green and red

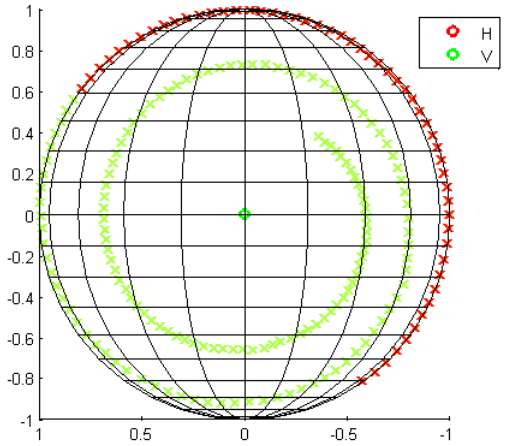

Figure 2. Received polarization of 200 received OFDM subchannels.

"x"s. The color of the marker is green if the subcarrier polarization state is on the front of the sphere (closer to the vertical polarization than horizontal) and red if the polarization state corresponds to the back of the sphere (closer to the horizontal polarization). We note that the dispersion pattern of the received signal is a spiral, which means that the amplitudes of the polarization components vary relative to one another as a function of frequency, indicating a frequency-selective channel.

The observed PMD, or frequency dependent polarization, can be explained by a simple two-path multipath model. Using two different delays and polarizations of the received multipath components, the resultant polarization will be a function of the relative phase between the two components, which is frequency dependent. In a more realistic multipath environment, the frequency dependent nature of the received polarization will still hold, though the dispersion may be more complicated.

III. Interference Mitigation Processing

For this analysis, two types of interference are used:

1. *Synthesized: an interference signal composed of white Gaussian noise with a bandwidth of 18 MHz*
2. *Collected: a rotated version of a second collected signal from the same experiment as the collected desired signal*

In a given simulation, one of these two signals is added to the received signal at complex baseband. For the first interference case, we force the polarization to be purely horizontal. Although simplistic, this polarization dispersion pattern allows us to examine certain trends in the processing algorithm described in this section. The second interference signal has a PMD associated with an actual channel and will be used to assess the algorithm's performance in a more realistic setting. The collected signal was rotated by the following matrix to more clearly demonstrate separability.

$$\begin{bmatrix} V' \\ H' \end{bmatrix} = \begin{bmatrix} cos(\pi/4) & sin(\pi/4) \\ -sin(\pi/4) & cos(\pi/4) \end{bmatrix} \begin{bmatrix} V \\ H \end{bmatrix} \quad (1)$$

where V and H represent the collected vertical and horizontal components and V' and H' the rotated components. This rotation shifts the PMD 90° around the Poincaré sphere.

OFDM Subchannel MMSE Filter

Assume the received data has the form

$$\vec{y} = \vec{h}_d x_d + \vec{h}_I x_I + \vec{n} \tag{2}$$

where $\vec{y}$, $\vec{h}_d$, $\vec{h}_I$, and $\vec{n}$ are 2x1 vectors associated with the horizontal and vertical elements of the received data, desired signal and interference complex channel gains, and noise respectively. x_d and x_I are the transmitted desired and interference signals.

The output of the processing is given by applying a weight vector to the received data

$$\hat{x}_d = \vec{w}^H \vec{y} \tag{3}$$

Using the channel estimates from the desired signal and the known channel information from the synthesized interference, the minimum mean squared error (MMSE) weight vector is calculated for each subcarrier using (4).

$$\vec{w}_{opt} = R_{yy}^{-1} \vec{r}_{yd} \tag{4}$$

The autocorrelation matrix (R_{yy}) and cross-correlation vector ($\vec{r}_{yd}$) are given by

$$\begin{aligned} R_{yy} &= E(\vec{y}\vec{y}^H) = P_d \vec{h}_d \vec{h}_d^H + P_I \vec{h}_I \vec{h}_I^H + \sigma^2 I \\ \vec{r}_{yd} &= E(\vec{y} x_d^H) = P_d \vec{h}_d \end{aligned} \tag{5}$$

where P_d and P_I are the average desired and interference signal powers, σ^2 is the noise power, and I is the identity matrix. Because we have not been rigorous in estimating the SNR, the noise power in this case is unknown, so for simplicity in our analysis, we set $\sigma^2 = 0$. This is equivalent to a zero-forcing filter as a special case of the MMSE solution.

Channel estimates for each of the subcarriers are used to determine $\vec{h}_d$; P_I and $\vec{h}_I$ are given by the parameters used to synthesize the interference. For the collected interference case, $\vec{h}_I$ is given by the channel estimates of the collected signal. Weight vectors are computed and applied for each subcarrier and then channel equalization is performed to yield soft decisions. Notice that this method assumes knowledge of the channel state information for both the desired signal and the interference. This requirement may be relaxed by estimating (5) using time averaging over a known training sequence. This simplification is not analyzed here, but is expected to perform slightly worse than the algorithm just described.

Suboptimal Full-band Polarization Filter

A suboptimal processing algorithm is also computed at one point to compare with full-band processing techniques. This is done by computing a single weight vector to be applied to all subcarriers. This is done by $\vec{w}_{sub} = \bar{R}_{yy}^{-1} \overline{\vec{r}_{yd}}$ where $\bar{R}_{yy}$ and $\overline{\vec{r}_{yd}}$ are averages of the R_{yy} and $\vec{r}_{yd}$ over all 200 subcarriers.

IV. Results

The following outlines the results of the investigation using the MMSE filter described above. The soft decisions of the desired OFDM signal are shown before and after filtering followed by some plots showing the polarization selected by the weight vectors.

Unless otherwise noted, this section reports results using the synthesized interference case. Near the end of the section, the collected interference case is analyzed.

OFDM Subchannel MMSE Filter

Figure 3 shows the soft decision outputs of the horizontal element after channel equalization when interference is present. The average signal-to-interference ratio (SIR) including the power from both antennas was approximately 0dB. The red dots indicate symbol errors.

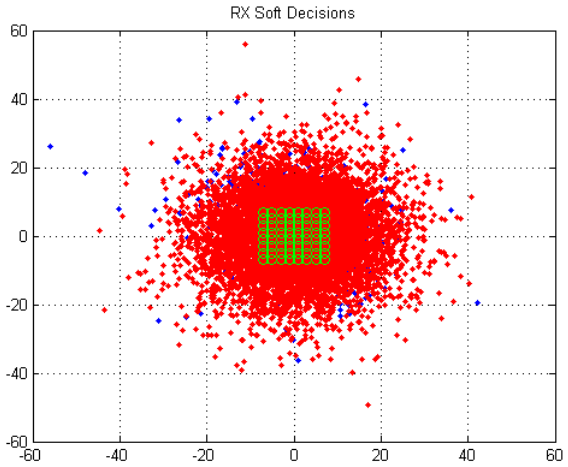

Figure 3. Soft decisions of a single OFDM frame with interference for horizontal receive polarization. Red dots indicate symbol errors.

By applying the MMSE filter weights to the various subcarriers and then equalizing the channel, the interference is suppressed and the desired signal soft decisions are recovered and plotted in Figure 4.

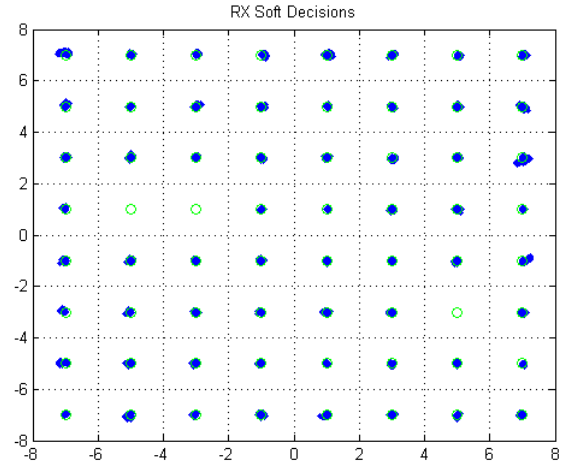

Figure 4. Soft decisions of a single OFDM frame with interference after polarization filtering.

Poincaré Sphere Analysis

By plotting the polarization of the weight vectors of the various subchannels, we can gain an intuitive understanding of what the MMSE filter is doing. Figure 5 shows the weight vector polarizations for the 200 subcarriers for three different values of SIR. When the interference power is extremely low (SIR = 60dB, which may put the interference close to or below the noise floor for this experiment), the weight vectors select polarizations very close to the polarization states of the desired signal subcarriers and the adaptive filter comes close to maximizing the polarization coupling of the desired signal. As the interference power increases, the polarization of each of the filter weight vectors gravitates toward the polarization orthogonal to the interference. Since the synthesized interference was fixed at pure horizontal, we see the weight vector polarizations begin to gravitate toward the vertical polarization on the front of the sphere. At SIR values less than roughly 30dB (representing a very low power interferer), the polarization state of the weights are almost purely orthogonal to the polarization of the interference in each subcarrier.

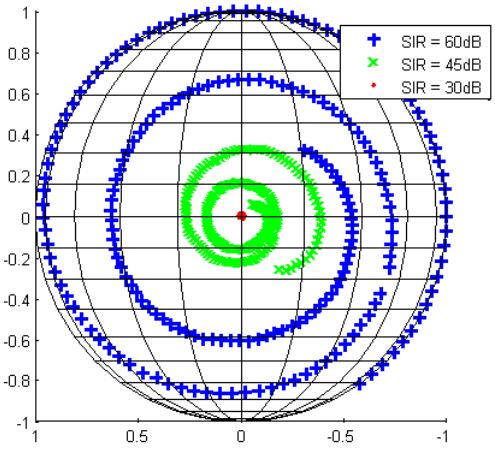

Figure 5. Weight vector polarizations for 200 OFDM subchannels with various SIR levels.

Another result of interest is that for each subcarrier, the polarization selected by the weight vector will lie on an arc drawn between the interference polarization and the point on the opposite end of the sphere that passes through the desired signal's polarization. In other words, given a single subcarrier, assume the interference polarization is given by the point p_d and the interference by p_i. The polarization orthogonal to p_i is given by $p_i^{\perp}$. The weight vector polarization will lie somewhere along the arc between p_d and $p_i^{\perp}$. The arc is illustrated in Figure 6 using collected data by plotting the polarizations of the weight vectors associated with a single OFDM subcarrier for 5 different SIR values. When SIR = 60dB, the weight vector polarization is very close to the desired signal polarization. As the SIR is reduced, the polarization slides along the great arc toward the polarization that is orthogonal to the interference on the subcarrier. Only one subcarrier is shown in the plot, but the phenomenon was verified for all 200 subcarriers for several values of SIR.

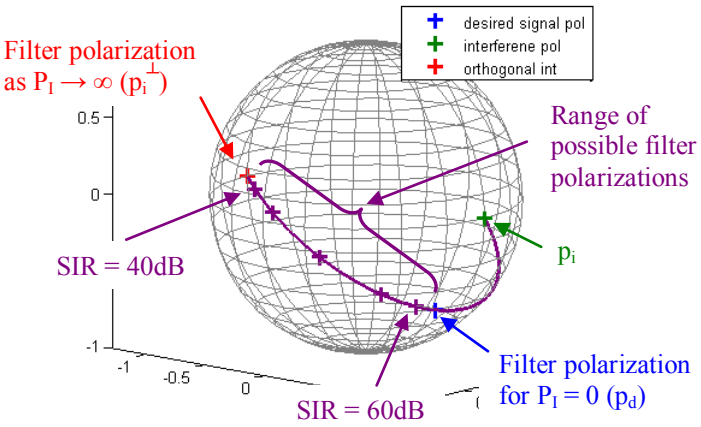

Figure 6. Weight vector polarizations for one OFDM subchannel with SIR levels ranging from 60dB to 40dB in 5dB steps. The purple arc shows the range of polarizations that may be chosen by the MMSE filter depending on the interference power.

When the interference power is zero, the polarization is selected to yield the maximum signal power. Since power couples as $cos^2\left(\frac{\gamma}{2}\right)$, where γ is the arc length between the two points, the filter selects the polarization where $\gamma = 0$. As the interference power grows larger, the filter will move toward selecting the polarization that is orthogonal to the interference in order to null it. It balances this against the estimated noise power in order to maximize the signal to interference plus noise ratio (SINR). When the filter is nulling the interference, if the desired signal polarization is close to that of the interference, then the arc length between the desired signal and filter polarizations will be close to π, the power coupling will be close to zero, and the SINR will be low. By adding spatial processing, this problem could be overcome assuming the two signals have different angles of arrival. When the two signals have the same incident angle and the same polarization, space-polarization processing will not be able to cancel the interference [2]. It seems likely, given the PMD observed for typical wireless channels, that such overlap would be limited to a small portion of the band. In an OFDM system, it may be possible to correct these low SINR subcarriers through forward error correction coding.

The result illustrated in Figure 6 was also observed by Stapor [9], who performs a theoretical analysis to determine the maximum SINR for the problem of co-channel interference mitigation using polarization processing. This analysis substantiates his conclusion with collected data and extends the concept to frequency-domain interference cancellation using OFDM.

Symbol Error Rate Analysis

Using collected data from a different dual-pol collection to simulate co-channel interference, symbol error rates were computed as a function of input SIR. Sub-band and full-band processing are plotted for comparison along with the results when the vertically polarized output is used (no filtering). The SIR gains for the two filtering techniques are approximately 60dB and 12dB respectively. Figure 7 shows the PMD of the

simulated interference signal. Again, the horizontal polarization is hidden from view and the points plotted are on the back side of the sphere (closer to horizontal than vertical).

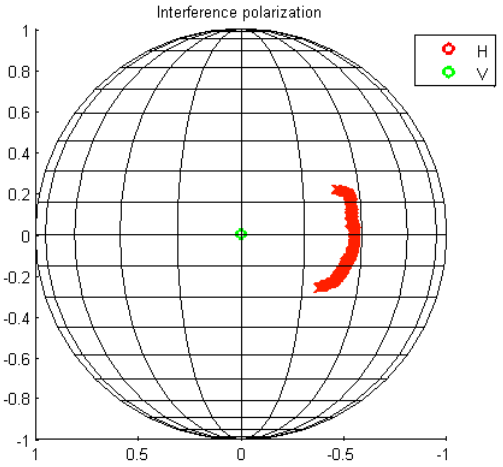

Figure 7. PMD of collected interference signal.

Figure 8 shows the estimated SER for three different cases using optimal sub-band filtering, suboptimal full-band filtering, and vertical polarization selection (no filtering).

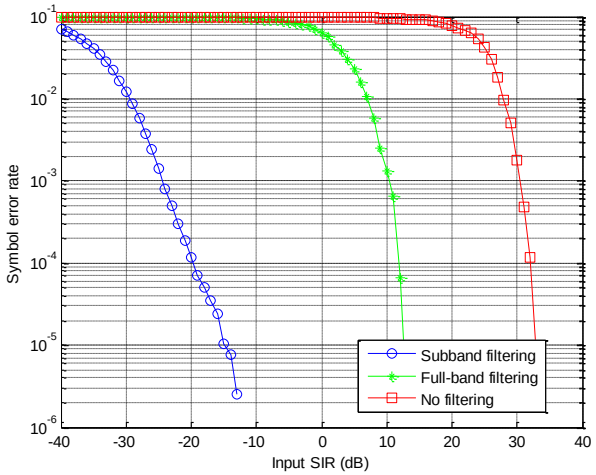

Figure 8. SER curves as a function of input SIR

The sub-band filtering method has an improvement over full-band filtering of anywhere between 25-40dB depending on the desired SER. Full-band filtering improves over vertical selection by about 20dB. These values of improvement are specific to the given configuration, but the general trends are clear and the utility of the sub-band filtering method is demonstrated.

V. Conclusion

Polarization-based processing for interference mitigation has been explored previously; however, sub-band polarization processing has not been extensively considered and is found to perform much better than a single polarization selection for the entire band. This is due to the observed polarization mode dispersion of a short-range indoor wireless channel. The PMD can be exploited when the polarization is selected on a subcarrier by subcarrier basis.

We report the observation of PMD in typical indoor wireless channels and propose the existence of the phenomenon in more general environments based on a brief discussion of a two-path multipath model. This paper also offers the technique of sub-band based polarization processing to exploit this PMD. Though OFDM is used to demonstrate the concept, the sub-banding technique may be applied more generally. If the signal is broadband relative to the inverse of the maximum delay spread of the channel, sub-band processing should yield improved performance relative to full-band filtering. OFDM lends itself well to this type of processing, but the technique may be used more generally with some additional processing.

A geometric interpretation of the selected polarization corresponding to the MMSE filter weights is also given using the Poincaré sphere. Though noted previously from a theoretical analysis [9], we offer an experimental validation of this result and extend it to consider frequency-polarization filtering. When the interference power is very small, the filter selects the polarization of the desired signal. As the interference power becomes larger, the filter weights move along a great arc of the sphere toward the polarization orthogonal to the interference.

Disclaimer

The views and conclusions contained in this document are those of the authors and should not be interpreted as representing the official policies, either expressed or implied, of the Army Research Laboratory or the U. S. Government.

References

1. ETSI 3GPP TR 25.996 Technical Report version 6.1.0 Release 6, "Universal mobile telecommunications system (UMTS); spatial channel model for multiple input multiple output (MIMO) simulations", p. 23, Sept 2003.
2. R. Compton, "On the performance of a polarization sensitive adaptive array", *IEEE Transactions on Antennas and Propagation*, vol. AP-29, No. 5, Sept 1981.
3. G. Zhang, Y. Liu, "Separation method of polarization states", *IEE Proceedings Radar, Sonar, and Navigation*, vol 147, pp 75-79, Apr 2000.
4. M. Takahashi, M., H. Takahashi, T. Tanaka, "Cross polarization interference canceler for microcellular mobile communication systems", *IEEE International Conference on Communication*, vol 2, pp 910-914, Jun 1995.
5. H.A. Mirza, M.M. Ahmed, "Interference rejection capability of cross dipole antenna array system", *International Conference on Advances in Space Technologies*, pp 68-74, Sep 2006.
6. A.J. Gasiewski, M. Klein, A. Yevgrafov, V. Leuskiy, V, "Interference mitigation in passive microwave radiometry", IEEE International Geoscience and Remote Sensing Symposium, vol 3, pp 1682-1684, Jun 2002.
7. R. Fante, "Principles of adaptive space-time-polarization cancellation of broadband interference", published by *The Mitre Corporation*, http://www.mitre.org/work/tech_papers/tech_papers_04/fante_adaptive/fante_adaptive.pdf
8. W. Xiang, P. Richardson, B. Walkenhorst, X. Wang and T. Pratt, "A high-speed four-transmitter four-receiver MIMO OFDM testbed: experiment results and analyses", *EURASIP Journal of Applied Signal Processing*, April 2006.
9. D. Stapor, "Optimal receive antenna polarization in the presence of interference and noise", *IEEE Transactions on Antennas and Propagation*, vol. 43, no. 5, May 1995.
10. T. Svantesson, M. Jensen, J. Wallace, "Analysis of electromagnetic field polarizations in multiantenna systems", *IEEE Trans. On Wireless Communications*, vol. 3, pp. 641-646, March 2004.